Yuzuncu Yil University Journal of the Institute of Natural & Applied Sciences

https://dergipark.org.tr/en/pub/yyufbed

Research Article

Numerical Analysis of Wind-Generated Circulation and Water Surface Changes: The Van Lake Case

Muhammet Ensar YİĞİT[1*]

[1]Manisa Celal Bayar University, Engineering and Natural Science Faculty, Civil Engineering Department, Manisa, Türkiye

*Corresponding author e-mail: ensar.yigit@cbu.edu.tr

Abstract: The computation of wind-induced fluid circulation in seas, bays and lakes is important for construction and commercial activities. Future scenarios under different conditions can be analyzed using a mathematical model and appropriate solution methods, which can be a guide for design and operational processes. In this study, a two-dimensional mathematical model for wind-induced surface circulation is developed by considering the bottom and surface boundary conditions, flow conditions and wind-fluid interaction. The general form of the equation is adapted for numerical analysis using finite difference expansion. Unlike the approaches in the literature that focus only on packaged circulation models, this study presents finite difference expansions and a solution method to enable researchers to perform similar analyses in different water masses. The model is customized using Lake Van data, including the digital depth map. Then, fluid circulation under varying wind directions and intensities is analyzed. The mathematical model examines surface change patterns and flow velocities based on predefined initial and boundary conditions. The obtained results are given with diagrams and graphs. This method applied to Lake Van can be applied to lakes, bays and seas of different sizes and plans.

Keywords: Fluid mechanics, Hydromechanics, Wind-generated circulation, Finite difference analysis, Lake Van circulation

Rüzgâr Kaynaklı Dolaşım ve Su Yüzeyi Değişimlerinin Sayısal Analizi: Van Gölü Örneği

Öz: Deniz, koy ve göllerde rüzgâr kaynaklı akışkan sirkülasyonunun hesaplanabilirliği, inşaat ve ticari faaliyetler için önemlidir. Farklı koşullar altındaki gelecekteki senaryolar, matematiksel bir model ve uygun çözüm yöntemleri kullanılarak analiz edilebilir ve bu da tasarım ve operasyonel süreçler için bir kılavuz olabilir. Bu çalışmada, taban ve yüzey sınır koşulları, akış koşulları ve rüzgâr-akışkan etkileşimi dikkate alınarak rüzgâr kaynaklı yüzey sirkülasyonu için iki boyutlu bir matematiksel model geliştirilmiştir. Denklemin genel biçimi, sonlu fark genişlemesi kullanılarak sayısal analiz için uyarlanmıştır. Literatürdeki yalnızca paketlenmiş sirkülasyon modellerine odaklanan yaklaşımların aksine, bu çalışma araştırmacıların farklı su kütlelerinde benzer analizler yapmalarını sağlamak için sonlu fark genişlemeleri ve bir çözüm yöntemi sunmaktadır. Model, dijital derinlik haritasını da içerecek şekilde Van Gölü verileri kullanılarak özelleştirilmiştir. Daha sonra, değişen rüzgâr yönleri ve şiddetleri altındaki akışkan sirkülasyonu analiz edilmiştir. Matematiksel model, önceden tanımlanmış başlangıç ve sınır koşullarına dayalı olarak yüzey değişim desenlerini ve akış hızlarını incelemiştir. Elde edilen sonuçlar diyagram ve grafiklerle verilmiştir. Van Gölü için uygulanan bu yöntem, farklı ölçülerdeki ve plandaki göller, körfezler ve denizler içinde uygulanabilir.

Anahtar Kelimeler: Akışkanlar mekaniği, Hidromekanik, Rüzgâr kökenli sirkülasyon, Sonlu farklar analizi, Van Gölü sirkülasyon

Received Date: 24.10.2025
Accepted Date: 12.02.2026

How to cited: Yiğit, M.E. (2026). Numerical Analysis of Wind-Generated Circulation and Water Surface Changes: The Van Lake Case. *Yuzuncu Yil University Journal of the Institute of Natural and Applied Sciences,, 31* 175-188. https://doi.org/10.53433/yyufbed.1778832

1. Introduction

Lakes and seas are water masses that are subject to important hydrodynamic processes under the influence of winds. The mobility on the surface of these water masses directly affects ecosystem dynamics by affecting the distribution of temperature, salinity, and other physical parameters. Wind-driven circulation is a motion/process that spreads from the surface layers of the water mass to its depths, and changes especially depending on the direction, speed, and continuity of the wind. The force that causes the circulation movement is the shear stress between the free water surface and the wind due to the movement of the wind, and circulation occurs with the movement of the fluid water surface (Csanady, 2001; Holthuijsen, 2007). This circulation, which occurs under the influence of wind, leads to various changes on the water surface and especially affects factors such as surface currents, wave sizes, water level increase and evaporation, which develop parallel to the direction of the wind (Figure 1). Circulation dynamics are of critical importance for various environmental sustainability and engineering applications. The effects of wind on the water surface can have important consequences in a wide range of areas such as marine ecosystems, fisheries, and climate change. It should also be noted that these movements in the water mass are of critical importance for monitoring water quality and the accuracy of hydrological models. In this context, a more detailed study of the effects of wind-induced dynamics on the physical properties of the water mass is of great importance for environmental management and sustainable use. This article aims to examine the mechanisms of wind-induced circulations and dynamic changes on the water surface in lake and marine ecosystems and to discuss the effects of these processes on environmental interactions. It conducts research on the multifaceted effects of wind irregularity, wave interaction, eddy viscosity distribution and shear stress on circulation patterns.

Figure 1. Storms in seas and lakes, a) Wind-generated waves (URL-1, 2024), b) Waves in Lake Van (URL-2, 2024).

Literature studies conducted to investigate wind-induced circulation processes and changes in water surface in lakes and seas were reviewed and summarized below.

Kiran et al. (1995) created a two-dimensional single-layer hydrodynamic model of the Black Sea in which currents are driven by the wind forcing effect. He used an open finite difference scheme where the equations are separated on a regular 128 x 79 grid. As a result, it was stated that some of the well-known circulation patterns in the seas were successfully simulated. Koçyiğit et al. (2004) presented the results of various circulation scenarios for wind-induced currents in a small lake with constant depth and changing topography. The numerical model developed can simulate wind-driven circulation in shallow, enclosed water masses, and the influence of topography and wind stress on the circulation pattern is of primary importance, while the non-hydrostatic pressure component has little effect. Bennington et al. (2010) used a hydrodynamic model over Lake Superior. As a result, surface circulation patterns mimic wind directions in winter, but become organized by the presence of thermal gradients in summer. Model results show that the increase in lake surface temperature (0.37°C/decade) is significantly associated with increases in wind speed over the lake (0.18 m/s/decade), increasing current velocities (0.37 cm/s/decade), and decreasing ice cover (-886 km^2/year). Zafirakou et al. (2014) presented a method for the optimization of stations combating oil spills in the coastal basin. He based his methodology on annual simulation of circulation in the basin according to climatic data and many choices such as oil spill simulation with Lagrangian particle method. Schoen et al. (2014) stated in their study that wind-driven circulation patterns and associated water exchanges drive important bio-hydrodynamic interactions in shallow lakes and estuaries. He stated that water exchange time scales are not homogeneous, with some basin ends having relatively long residence times. Zafirakou, et al. (2015) in their study, have discussed in detail the oil spill numerical model and a 3D hydrodynamic model that simulate the transport and erosion of an oil spill (due to a series of physio-chemical processes that develop over time) in a coastal area. The findings of the present study emphasize the experience on the subject and show that such models can be applied in tracking the source of a spill or predicting its path and propagation, thus being valuable in real-time crisis management. Santo et al. (2017) in their study investigated the wind-induced circulation in a peri-alpine lake. The analysis of eddy viscosities showed significant differences compared to the oceanic case characterized by the absence of coastal boundaries and homogeneous, steady wind. In the case of non-homogeneous wind, the up flow and downflow areas are not only limited along the coastline, but also generated in the water mass due to significant horizontal velocity deviation, and the eddy viscosities indicated that turbulent mixing measured by the dissipation ratio appears to be more enhanced than in the case of homogeneous wind. Swatridge et al. (2022), in their study, indicated that the wind-driven nature of large lakes makes accurate meteorological inputs essential for hydrodynamic modelling. To investigate large lakes under wind influence, they applied a model to simulate the fluctuations and circulation in two different storms. Simulations that included vertical density gradients provided a better representation of current speeds with depth, allowing better prediction of peak storm wave magnitudes and surface water level behaviour following storms. Dangin et al. (2024) reported that surface water currents and waves are largely driven by the shear stress exerted on the water surface by the wind. In his study, he simulated the hydrodynamics of the Bay using high-resolution wind data as input and compared the results with the use of uniformly directed wind. As a result, he stated that global weather inputs can be used in areas with sparse monitoring stations, if they are validated. Zhang et al (2024) stated that wind is a critical driver in hydrodynamic and water quality modelling of large shallow lakes. He stated that contemporary empirical formulas for estimating the drag coefficient Cd are inadequate in inland lake models and often lead to underestimation of water speed. In general, the wave-dependent Cd formula provides an improvement in the surface circulation in the model and will improve the management of lake ecosystems.

Although there are biological, chemical, seismic, and geological studies on Lake Van in the literature, it has been observed that research on wind-based fluid circulation is limited. In this context, it is hoped that this study will pioneer circulation research on Lake Van.

2. Material and Methods

2.1. Coastal circulation

The driving force behind circulation in geophysical domains lies in the shear stresses exerted by wind on the water surface. These shear stresses are fundamental components of the model, manifested as free surface boundary conditions. In smaller-scale geophysical domains, characterized by lengths on the order of 10^4 m, the assumption of uniform wind velocity allows for the treatment of shear stress components (τ_{sx} and τ_{sy}) as spatially constant but temporally variable (Gill, 1982; Cushman-Roisin, & Beckers, 2011). However, as domain sizes increase, this assumption becomes less tenable, necessitating a rigorous examination of wind nonuniformity effects.

While this study does not provide a comprehensive solution to the general circulation problem, it offers valuable insights into the distribution of eddy viscosity across the vertical domain. Notably, stronger velocity gradients near both the bed and the water surface intensify turbulence and vertical momentum diffusion (Pope, 2000). This relationship is intricately linked to both the bottom velocity (u_b^*) and the velocity at the water surface ($u_s^* = \sqrt{\tau_s/\rho}$) (Koutitas, 1988).

The distribution of eddy viscosity, derived from higher-order turbulence closure, provides a nuanced representation of the wind-generated profile. An important observation is the maximal eddy viscosity occurring at a distance of $\frac{1}{3}h$ from the water surface, with h representing the water depth (Rodi, 1993). The value of maximal eddy viscosity is proportionally tied to Equation 1, encapsulating the intricate relationship between wind characteristics and water circulation (Koutitas, 1988).

$$\nu_{max} \propto \lambda u_s \times h, \qquad O[\lambda] = 0.1 \tag{1}$$

In geophysical areas laterally bounded by coastal boundaries, the direction and intensity of currents vary significantly with depth. At the surface, currents align with the prevailing wind direction, a phenomenon characterized by a deflection to the right in the northern hemisphere due to the Coriolis effect (Gill, 1982; Pedlosky, 1987). Below the surface, however, a significant reversal in current direction occurs due to return flows caused by coastal boundaries.

2.2. Mathematical model development

Observations of the general morphology of wind-generated current profiles highlight the need for careful consideration when using simple depth-averaging techniques. Historically, the simple approach of applying a two-dimensional horizontal (2DH) model to the wind-generated circulation has been common (Koutitas 1988; Falconer, 1992). However, it is imperative to exercise caution and recognize the limitations inherent in such methodologies.

In contrast to the simple depth averaging commonly used in models, the complexities inherent in wind-generated current profiles require a more nuanced approach. The two-dimensional horizontal model frequently used in operational contexts, as in the following equations (Falconer, 1992; US Army Corps of Engineers, 2016):

$$\frac{\partial U}{\partial t} + U\frac{\partial U}{\partial x} + V\frac{\partial U}{\partial y} = -g\frac{\partial \zeta}{\partial x} + fV + \frac{\tau_{sx}}{\rho h} - \frac{\tau_{bx}}{\rho h} \tag{2}$$

$$\frac{\partial V}{\partial t} + U\frac{\partial V}{\partial x} + V\frac{\partial V}{\partial y} = -g\frac{\partial \zeta}{\partial y} - fV + \frac{\tau_{sy}}{\rho h} - \frac{\tau_{by}}{\rho h} \tag{3}$$

$$\frac{\partial \zeta}{\partial t} + \frac{\partial (Uh)}{\partial x} + \frac{\partial (Vh)}{\partial x} = 0 \tag{4}$$

In Kutitas (1988) work, detailed programming was made by considering the free surface condition, bed condition and depth average speed condition. As a result, the horizontal momentum distribution for wind-driven circulation and the improved 2DH model for bearing friction are given below.

$$\frac{\partial U}{\partial t} + U\frac{\partial U}{\partial x} + V\frac{\partial U}{\partial y} + \left(0.2U + \frac{a_x}{40}\right)\frac{\partial U}{\partial x} + \left(0.2V + \frac{a_y}{40}\right)\frac{\partial U}{\partial y} = -g\frac{\partial \zeta}{\partial x} + fV + \frac{\tau_{sx}}{\rho h} - \left(0.18\frac{U}{h}\sqrt{\frac{\tau_s}{\rho h}} - 0.5\frac{\tau_{sx}}{\rho h}\right) \tag{5}$$

$$\frac{\partial V}{\partial t} + U\frac{\partial V}{\partial x} + V\frac{\partial V}{\partial y} + \left(0.2U + \frac{a_x}{40}\right)\frac{\partial V}{\partial x} + \left(0.2V + \frac{a_y}{40}\right)\frac{\partial U}{\partial y} = -g\frac{\partial \zeta}{\partial x} - fV + \frac{\tau_{sy}}{\rho h} - \left(0.18\frac{V}{h}\sqrt{\frac{\tau_s}{\rho h}} - 0.5\frac{\tau_{sy}}{\rho h}\right) \tag{6}$$

Coastal boundary conditions are given in detail in the study of Koutitas (1988). The only variation appears in the statements for the computation of U, V (the velocity components) and in the application of the open-sea boundary condition. The wind influence is assumed constant over the circulation. A time series of wind velocity components could be introduced in the case of wind varying with time. The initial condition is one of a cold start and the transient development of the hydrodynamic conditions to steady flow is followed. The printed results display U, V and ζ values at the mesh centers. Equation 7 permits the computation of the current pattern at any depth.

$$u(z) = \left(\frac{3}{4}a - \frac{3}{2}U\right)\left[\left(\frac{z}{h}\right)^2 - 1\right] + a\left(\frac{z}{h} + 1\right) \tag{7}$$

2.3. Modelling with finite differences

The application is a comparative presentation of the numerical solutions of the two 2DH models of wind generated circulation, the modified one and the classical one without correction of the $u(\partial u/\partial x)$, τ_b/ρ terms. In Figure 2.a (x, y) shows the change in position, (t) shows the change in time. Here; $U(x, y, t)$: shows the speed value in x direction, $V(x, y, t)$: shows the speed value in y direction, $\zeta(x, y, t)$: shows the change in water surface for stagnant water level (SWL).

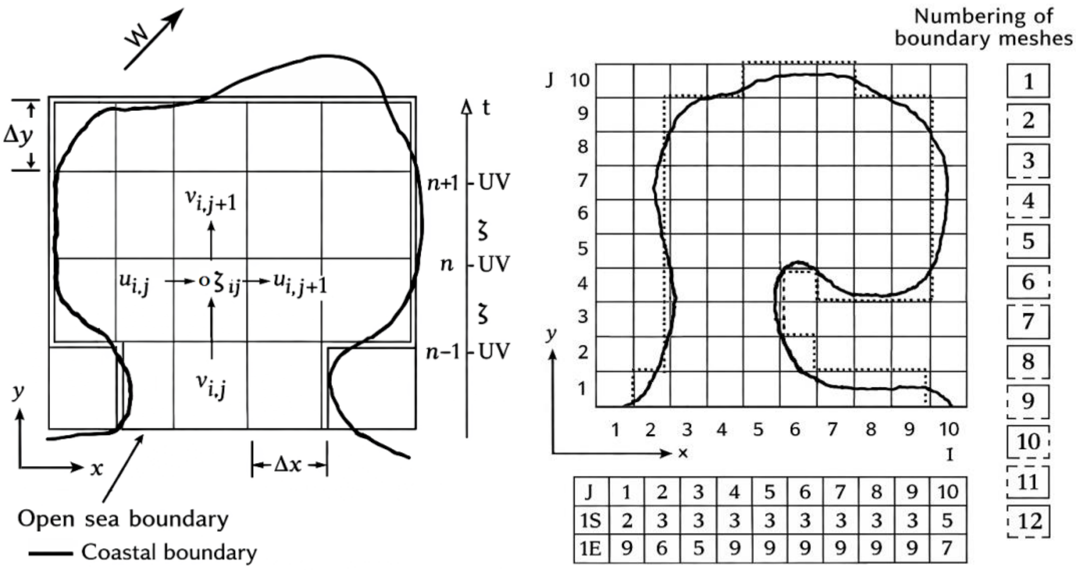

Figure 2. a) Orthogonal staggered grid for spatial and time discritisations, b) Morphology of coastal and typical boundary meshes (Koutitas, 1988).

The finite difference forms according to the current open scheme are given below. In the present study, the term 'open scheme' refers to the explicit finite difference method (FDM) employed for time integration, following the approach described by Koutitas (1988).

Representation of velocity change in x-direction by finite difference method;

$$VV = V_{(i,j)} + V_{(i-1,j)} + V_{(i,j+1)} + V_{(i-1,j+1)}/4 \tag{8}$$

$$AD = \left(1.2\,U_{(i,j)} + 0.4\,\mathrm{sign}(\tau_X)\sqrt{|\tau_X|}\right)\left(\frac{U_{(i+1,j)} - U_{(i-1,j)}}{2D_x}\right) + \left(1.2\,VV + 0.4\,\mathrm{sign}(\tau_y)\sqrt{|\tau_y|}\right)\left(\frac{U_{(i,j+1)} - U_{(i,j-1)}}{2D_x}\right) \tag{9}$$

$$BF = \left(0.18\,U_{(i,j)}\sqrt{\tau_S} - \frac{\tau_X}{2}\right)\Big/\left(\frac{H_{(i,j)} + H_{(i-1,j)}}{2}\right) \tag{10}$$

$$UN_{(i,j)} = U_{(i,j)} - D_T\left(AD + 9.81\left(\frac{\zeta_{(i,j)} - \zeta_{(i-1,j)}}{D_x}\right) - F\times VV + BF - \tau_X/\left(\frac{H_{(i,j)} + H_{(i-1,j)}}{2}\right)\right) \tag{11}$$

Representation of velocity change in y-direction by finite difference method;

$$UU = U_{(i,j)} + U_{(i+1,j)} + U_{(i,j-1)} + U_{(i+1,j-1)}/4 \tag{12}$$

$$\mathrm{AD} = \left(1.2\,\mathrm{U}_{(i,j)} + 0.4\,\mathrm{sign}(\tau_y)\sqrt{|\tau_y|}\right)\left(\frac{\mathrm{V}_{(i,j+1)} - \mathrm{V}_{(i,j-1)}}{2\mathrm{D}_x}\right) + \left(1.2\,\mathrm{UU} + 0.4\,\mathrm{sign}(\tau_x)\sqrt{|\tau_x|}\right)\left(\frac{\mathrm{V}_{(i+1,j)} - \mathrm{V}_{(i-1,j)}}{2\mathrm{D}_x}\right) \quad (13)$$

$$\mathrm{BF} = \left(0.18\,\mathrm{V}_{(i,j)}\sqrt{\tau_s} - \frac{\tau_y}{2}\right) / \left(\frac{\mathrm{H}_{(i,j)} + \mathrm{H}_{(i-1,j)}}{2}\right) \quad (14)$$

$$\mathrm{VN}_{(i,j)} = \mathrm{V}_{(i,j)} - \mathrm{D_T}\left(\mathrm{AD} + 9.81\left(\frac{\zeta_{(i,j)} - \zeta_{(i,j-1)}}{\mathrm{D_x}}\right) - \mathrm{F}{\times}\mathrm{UU} + \mathrm{BF} - \tau_y/\left(\frac{\mathrm{H}_{(i,j)} + \mathrm{H}_{(i-1,j)}}{2}\right)\right) \quad (15)$$

Representation of the level change on the water surface using the finite difference method;

$$\zeta_{(i,j)} = \zeta_{(i,j)} - \frac{\mathrm{D_T}}{2\mathrm{D_X}}\left(\begin{array}{c}\mathrm{U}_{(i+1,j)}\left(\mathrm{H}_{(i,j)} + \mathrm{H}_{(i+1,j)}\right) - \mathrm{U}_{(i,j)}\left(\mathrm{H}_{(i,j)} + \mathrm{H}_{(i-1,j)}\right) \\ -\mathrm{V}_{(i,j+1)}\left(\mathrm{H}_{(i,j)} + \mathrm{H}_{(i,j+1)}\right) - (\mathrm{V}_{(i,j)}\left(\mathrm{H}_{(i,j)} + \mathrm{H}_{(i,j-1)}\right)\end{array}\right) \quad (16)$$

Where: $\tau_x = C_s * W_x\sqrt{W_x^2 + W_y^2}$, $\tau_y = C_s * W_y\sqrt{W_x^2 + W_y^2}$, $\tau_s = \sqrt{\tau_x^2 + \tau_y^2}$, D_T: time discretization steps (in seconds), D_X: space discretization steps (m, $D_X = D_Y$), C_s: wind friction coefficient K, W_X: wind velocity components along Ox (m/s), W_Y: wind velocity components along Oy (m/s), IM: maximum values of I grid indices along x direction, JM: maximum values of J grid indices along y direction, F: Coriolis coefficient, KB: number of boundary (coastal+open sea) meshes to be specially treated, NM: maximum number of time steps. To perform analysis with the finite difference method, an algorithm was created in the Matlab prog. using the above equations (Eq. 8-16).

2.4. Features and boundary conditions

In order to distinguish between a terrestrial area and a lake or sea, the boundaries must be determined and the speed values at these boundaries must be introduced to the computer program (Figure 2.b). For this reason, the U and V speed boundary conditions that must be met for special grid cells (NB) are given in Table 1, taken from the study of Koutitas (1988).

Table 1. Special grid cell numbers (NB) and boundary conditions

NB	Velocity Limit Conditions	
1	$UN_{(i,j)} = 0;$	
2	$VN_{(i,j)} = 0;$	
3	$UN_{(i,j)} = 0;$	$VN_{(i,j)} = 0;$
4	$UN_{(i,j)} = -\zeta_{(i,j)}\sqrt{9.81/H_{(i,j)}};$	$VN_{(i-1,j)} = VN_{(i,j)}$
5	$UN_{(i+1,j)} = \zeta_{(i,j)}\sqrt{9.81/H_{(i,j)}};$	$VN_{(i+1,j)} = VN_{(i,j)}$
6	$VN_{(i,j+1)} = \zeta_{(i,j)}\sqrt{9.81/H_{(i,j)}};$	$UN_{(i+1,j)} = UN_{(i,j)}$
7	$VN_{(i,j)} = -\zeta_{(i,j)}\sqrt{9.81/H_{(i,j)}};$	$UN_{(i-1,j)} = UN_{(i,j)}$
8	$UN_{(i,j)} = -\zeta_{(i,j)}\sqrt{9.81/H_{(i,j)}};$	$VN_{(i,j)} = 0;$
9	$UN_{(i+1,j)} = \zeta_{(i,j)}\sqrt{9.81/H_{(i,j)}};$	$VN_{(i,j)} = 0;$
10	$UN_{(i,j)} = 0;$	$VN_{(i,j+1)} = \zeta_{(i,j)}\sqrt{9.81/H_{(i,j)}};$
11	$UN_{(i,j)} = 0;$	$VN_{(i,j)} = -\zeta_{(i,j)}\sqrt{9.81/H_{(i,j)}};$

3. Case Study

3.1. Chosen lake description

Lake Van is a volcanic dam lake formed approximately 200 thousand years ago as a result of the 60 km long lava that closed the tectonic depression area in the region as a result of the eruption of the Nemrut volcanic mountain within the borders of Van and Bitlis provinces (Figure 3.a,b). Lake Van, which has many bays, has a surface area of 3,713 km^2. Lake Van is an aquatic ecosystem that is different from both freshwater and marine ecosystems. Its waters are salty and soda. The salinity rate of the lake water is 19‰ and its pH is 9.8. For this reason, Lake Van does not freeze despite its high altitude and harsh winters. The lake water level rises and falls depending on the climate. However, its average height above sea level is 1646 meters. The average depth of the lake is 171 m and its deepest point is 451 meters. Recent studies have determined that the age of the lake is 600,000 years (Stockhecke et al. 2012; Stockhecke et al. 2014). Lake Van is the largest soda lake in the world and also the largest lake in Türkiye (Figure 4.a.b). The salty-soda waters of the lake limit biodiversity (Düzen, 2011; Akköprü et al. 2019).

Figure 3. a) Van Lake and Akdamar Church (URL-3, 2024), b) Van Lake view (URL-4, 2024).

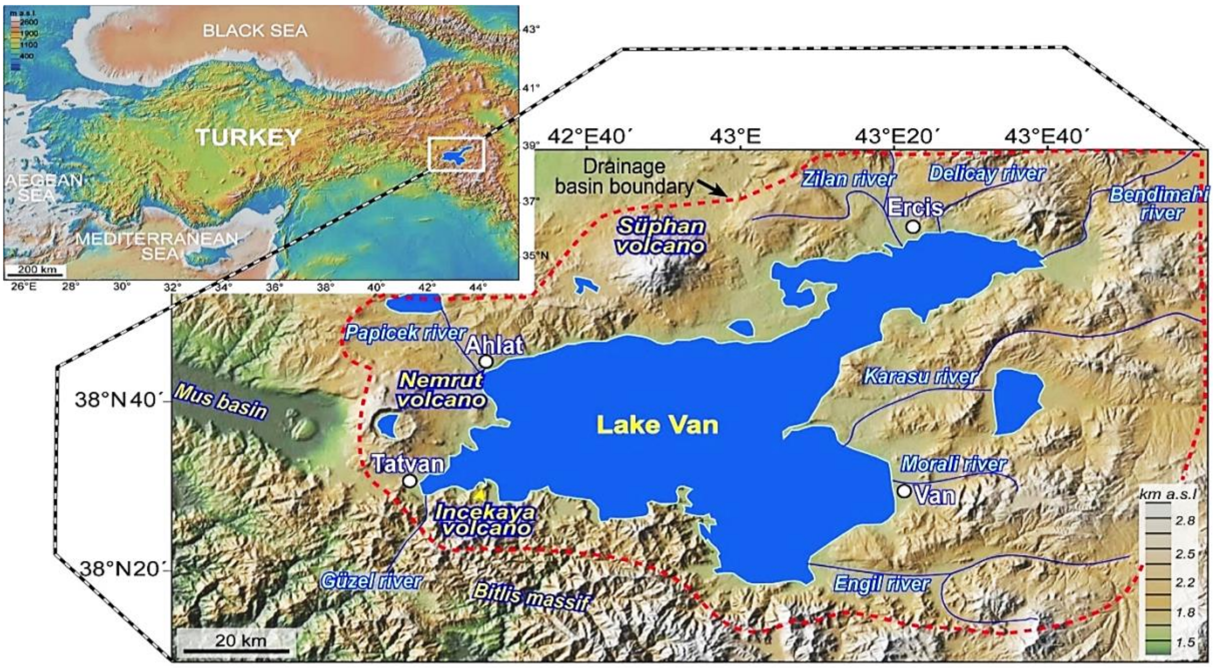

Figure 4. Map of the Republic of Türkiye and Lake Van detail (Cukur et al. 2014).

In this study, analyses were conducted for 8 different wind conditions that are likely to occur in the main and intermediate directions on Lake Van, given in Table 2. In all these cases, the wind speed was taken as a constant value to facilitate comparison. In Figure 5.a, the borders of Lake Van were determined, and the grid area was created. With the help of Figure 5.b, the change in the depth of the lake with the location was determined approximately and Table 5. was prepared.

Table 2. Analysis cases

Cases	W_x	W_y	Wind Direction
Case 1	10	10	Northeast
Case 2	-10	-10	Southwest
Case 3	-10	10	Northwest
Case 4	10	-10	Southeast
Case 5	0	10	North
Case 6	0	-10	South
Case 7	10	0	East
Case 8	-10	0	West

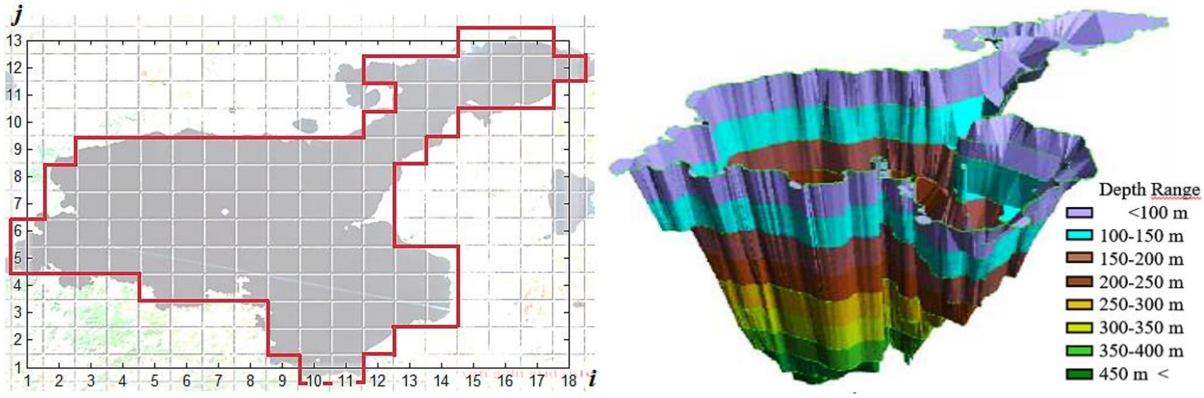

a) b)

Figure 5. a) Grid system and plan of Lake Van, b) Three-dimensional representation of Lake Van (Sarı, 2000).

3.2. Material properties and finite difference method boundary conditions

The accepted properties for lake water and wind in the modeling are given in Table 3 below. In addition, the properties such as position increment, time increment and number of steps required for the finite difference model are presented in the table. The lake boundaries required in the finite difference model are determined from Figure 5.a for each vertical grid (J) and the starting (IS) and ending (IE) points are given in Table 4 below. The depth values of Lake Van are read from Figure 5.b and written in Table 5. The boundary conditions (NB) for the special grid cells shown in Figure 2.b were given in Table 1 before. Accordingly, the determined boundary condition numbers are given in Table 6.

Table 3. Material properties (Yiğit & Yıldırım, 2025; Yiğit & Tuncer Uysal, 2023; Koutitas, 1988)

DT (s)	DX=DY (m)	CS	WX (m/s)	WY (m/s)	IM	JM	F	KB	NM
30	6000	$5x10^{-6}$	-10, 10	-10, 10	18	13	$1x10^{-4}$	23	1000

Table 4. Finite difference grid boundaries of Lake Van

J	1	2	3	4	5	6	7	8	9	10	11	12	13
IS	10	9	9	5	1	1	2	2	3	12	13	12	15
IE	11	12	14	14	14	12	12	12	13	14	17	18	17

Table 5. Depth values of Lake Van (H(m))

13															25	25	25	
12												25	25	25	50	50	50	25
11													50	75	25	25	25	
10												25	75	25				
9			25	25	25	50	50	50	50	50	50	100	25					
8		25	50	50	75	150	150	200	150	125	75	100						
7		25	100	100	150	250	350	350	300	225	125	100						
6	25	50	50	50	150	250	250	350	450	300	150	100						
5	25	25	25	25	75	150	150	200	300	225	125	100	25	25				
4					25	50	50	50	150	150	100	75	50	50				
3									50	100	75	50	25	25				
2									25	50	50	25						
1										25	25							
J / i	**1**	**2**	**3**	**4**	**5**	**6**	**7**	**8**	**9**	**10**	**11**	**12**	**13**	**14**	**15**	**16**	**17**	**18**

Table 6. Special meshes and their features

KB	1	2	3	4	5	6	7	8	9	10	11	12	13	14	15	16	17	18	19	20	21	22	23	24	25	26	27
IB	1	5	9	10	2	3	4	6	7	8	11	12	13	14	15	16	17	18	1	2	2	3	9	12	12	13	15
JB	5	4	2	1	5	5	5	4	4	4	1	2	3	3	11	11	11	12	6	7	8	9	3	10	12	11	13
NB	4	4	4	4	3	3	3	3	3	3	3	3	3	3	3	3	3	3	2	2	2	2	2	2	2	2	2

4. Results

The computer-aided analysis of finite difference equations with the Matlab Program revealed two different findings. The first is the contour maps showing the changes in water level differences with location due to the circulation on the lake surface due to winds blowing in different directions (Figures 6-7). The second is the graphs showing the temporal changes of water levels (maximum decrease or maximum increase) at the control points (Figure 8-9). The computer program can also calculate the velocity components (U,V) and energy (E) of the fluid on the lake surface. However, these outputs are not visualized in order to keep the number of pages of the study short.

The results of the numerical analyses performed according to the assumption of constant wind speeds show that the circulation and surface level amplitudes reach a steady state after a certain processing step (Figure 8-9). The accuracy of the model should be checked in longer processing times. When the analyses performed for the cases representing the intermediate directions (Case 1-4) are examined, it is calculated that the water level on the lake surface rises by approximately 0.126 m under the effect of the northeast wind (Case 1), while the other region drops by approximately -0.054 m. It is calculated that the water level on the lake surface rises by approximately 0.062 m under the effect of the southwest wind (Case 2), while the other region drops by approximately -0.110 m. It is calculated that the water level on the lake surface rises by approximately 0.083 m under the effect of the northwest wind (Case 3), while the other region drops by approximately -0.047 m. It is calculated that the water level on the lake surface rises by approximately 0.051 m under the effect of the southeast wind (Case 4), while the other region drops by approximately -0.078 m.

When the analyses performed for the cases representing the main directions (Case 5-8) are examined, it is calculated that the water level on the lake surface rises by approximately 0.046 m under the effect of the north wind (Case 5), while the other region falls by approximately -0.009 m. It is calculated that the water level on the lake surface rises by approximately 0.006 m under the effect of the south wind (Case 6), while the other region falls by approximately -0.045 m. It is calculated that the water level on the lake surface rises by approximately 0.062 m under the effect of the east wind (Case 7), while the other region falls by approximately -0.035 m. It is calculated that the water level on the lake surface rises by approximately 0.046 m under the effect of the west wind (Case 8), while the other region falls by approximately -0.044 m.

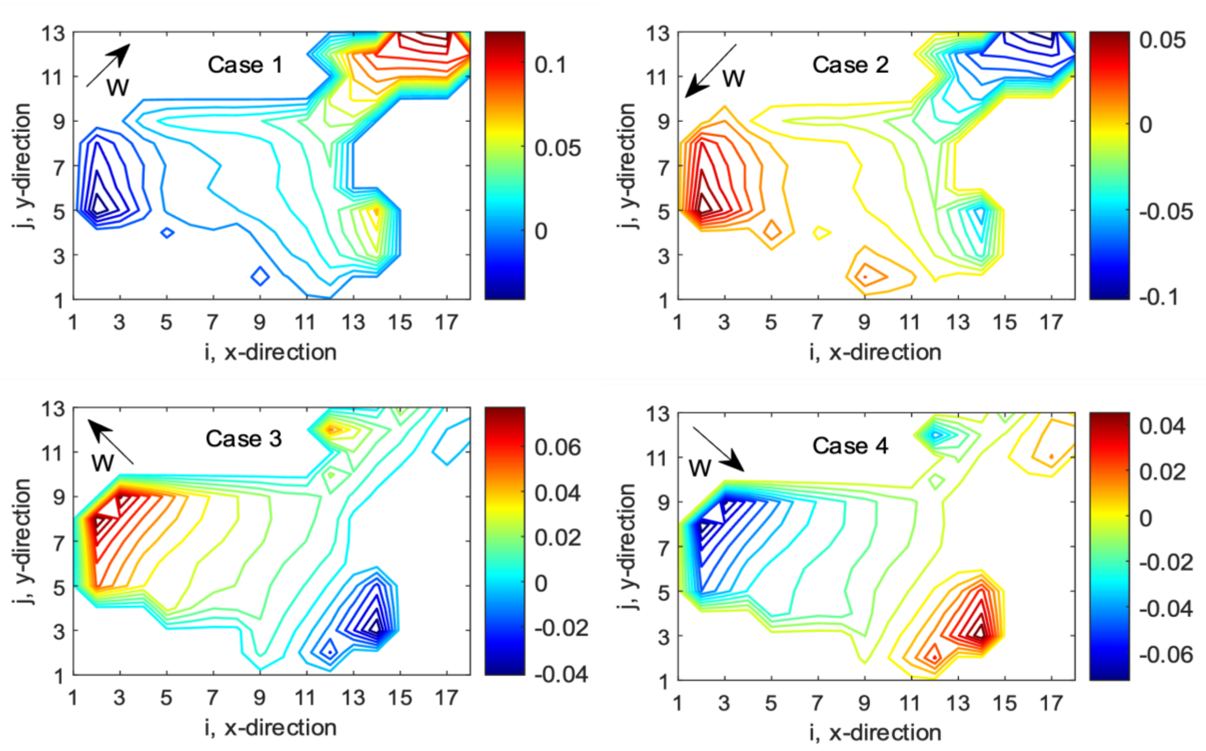

Figure 6. Isobath curves formed by wind for the determined intermediate direction cases (Case 1-4).

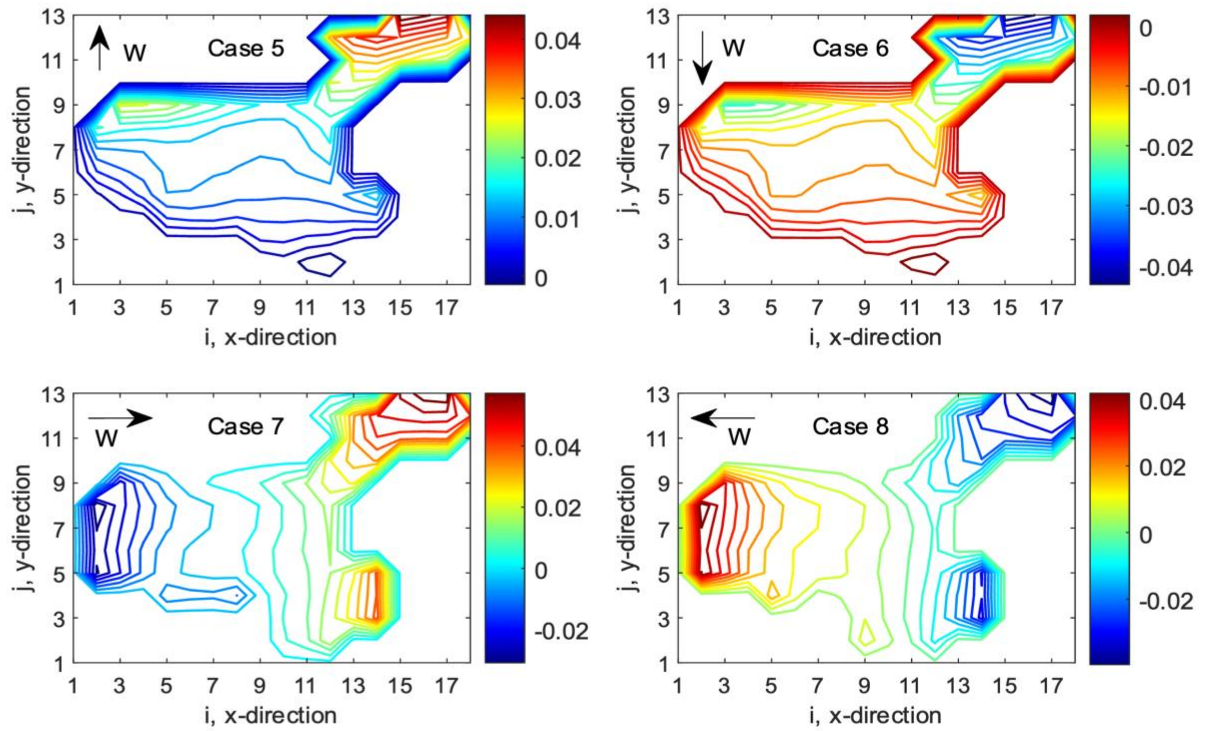

Figure 7. Isobath curves formed by wind for the determined main direction cases (Case 5-8).

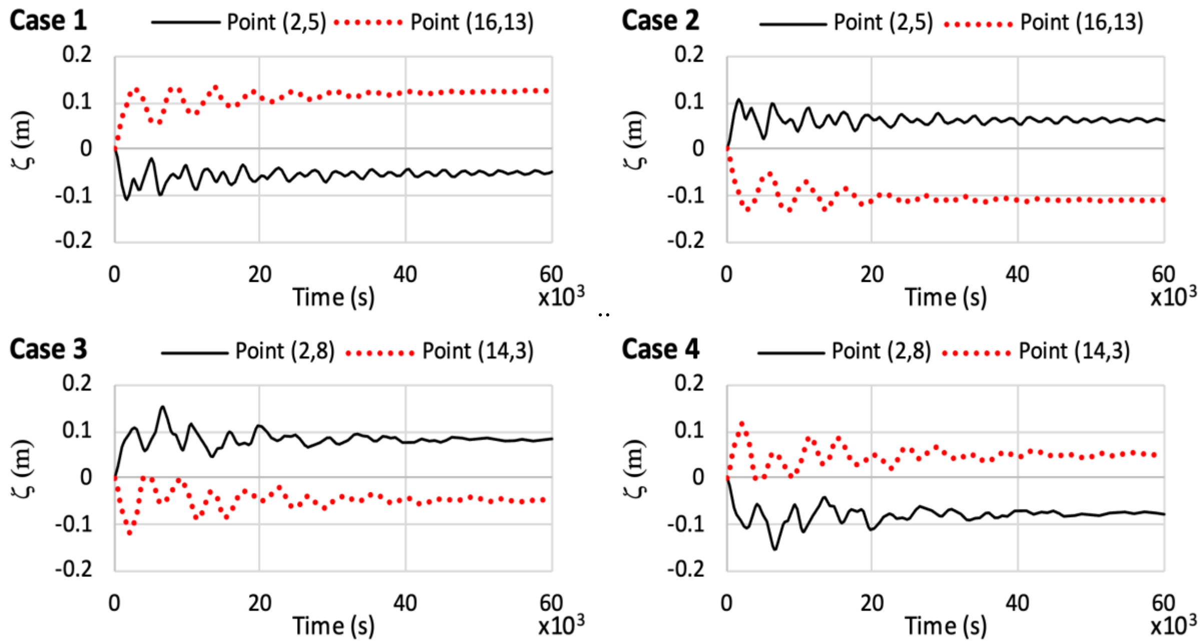

Figure 8. For cases 1-4, the maximum rise and fall changes of the water surface during the analysis period under intermediate wind conditions.

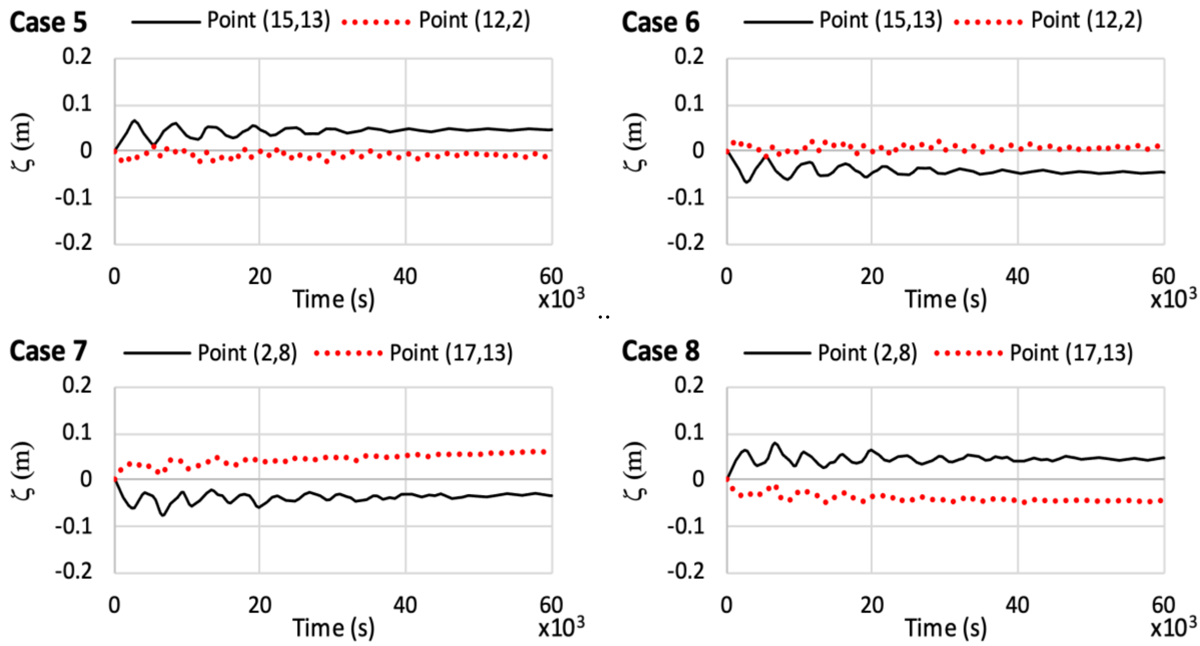

Figure 9. For cases 5-8, the maximum rise and fall changes of the water surface during the analysis period under main wind conditions.

5. Discussion and Conclusion

In this study, the interaction between the wind and the lake surface was investigated extensively and the mathematical model explaining the level differences along the water surface was examined with updated computer program codes. In addition, the level differences occurring at different points of the water surface were determined numerically. When the contour diagrams and time-varying graphs were examined, it was calculated that the rise or fall in the water level in the regions where the lake was shallow was greater than in the regions where the water was deep. When the time-varying graphs were examined, it was seen that the results reached a steady state after 40E3 seconds. It was determined that the highest water level rise occurred as a result of the wind blowing in the northeast direction, and the highest fall occurred as a result of the wind blowing in the southwest direction. The fact that the axis of the lake is in the northeast-southwest direction contributed to these results. On the northwest-southwest axis, the lake is approximately symmetrical. This caused the rise and fall in the water levels to be approximately similar values in the winds blowing in this direction. Since the calculation was made with the resultant speed in the intermediate directions, the results were greater than in the main directions. In addition, it has been determined that the decreases or increases in the areas where the surface of the lake is narrow, depending on the wind direction, are greater than in other areas where the surface is wide. It is understood that decreases or increases in large water masses have great effects on the small water masses connected to them. This shows that wind-based circulation will affect the bay or river connections in similar lakes more. As a suggestion for future research, mathematical models can be used to investigate the effects of water level changes in lakes for different wind speeds and to calculate the possible increase/decrease amounts. The accuracy of the mathematical model can be tested with longer-term analyses. In addition, calculations can be made with the mathematical model for wind speeds and directions that change over time, and the protection of coastal structures from possible floods can be examined.

Acknowledgements

In this study, the software provided by the project number 2024-047 supported by Manisa Celal Bayar University Scientific Research Projects Coordination Unit was used.

Congress and/or Thesis Statement
The study is not derived from any thesis or congress paper.

Author contributions
Muhammet Ensar YİĞİT: Draft Writing, Theory Formulation, Investigation, Formal Analysis, Visualization, Methodology, Supply of Resources/Materials/Tools, Data Analysis, Review & Editing.

Conflict of interest:
The authors declared no potential conflicts of interest with respect to the research, authorship, and/or publication of this article.

Statement on Research and Publication Ethics
The author declares that he obeys the research and publication ethics:
YÖK Scientific Research and Ethics Regulation (yok.gov.tr), Declaration of Helsinki, Commitee on Publication Ethics (COPE), WAME

Ethics Committee Declaration
The author declare that the materials and methods used in the article do not require ethics committee approval and/or special legal permission.

Statement on the Use of Artificial Intelligence
The author(s) declares(declare) that they have not used any form of generative artificial intelligence in writing this article, creating any images, graphs, tables, or related titles.

Data Availability
No database was used for the study.

References

Akköprü, E., Aydın F. A., & Doğu, A. F. (2019). Van Gölü seviye değişimlerinin Engil Çayı Deltası jeomorfolojisi üzerine etkisi ve Dilkaya Höyüğü ile ilişkisi. *Türk Coğrafya Dergisi,* 72, 45-51. https://doi.org/10.17211/tcd.536643

Bennington, V., McKinley, G. A., Kimura, N. & Wu, C. H. (2010). General circulation of Lake Superior: Mean, variability, and trends from 1979 to 2006. *Journal of Geophysical Research,* 115, 1-14. https://doi.org/10.1029/2010JC006261

Csanady, G.T. (2001). *Air–Sea Interaction: Laws and Mechanisms* (1st ed.). Cambridge University Press. https://doi.org/10.1017/CBO9781139164672

Cukur, D., Krastel, S., Schmincke, H. U., Sumita, M., Tomonaga, Y., & Çağatay, N.M. (2014). Water level changes in Lake Van, Turkey, during the past ca. 600 ka: climatic, volcanic and tectonic controls. *Journal of Paleolimnology*, 52, 201–214. https://doi.org/10.1007/s10933-014-9788-0

Cushman-Roisin, B. & Beckers, J.-M. (2011). *Introduction to Geophysical Fluid Dynamics: Physical and Numerical Aspect* (2nd ed.), Academic Press.

Dangin, M. R., Sumagaysay, L. A., Herrera, E. C., & Bilang, R. G. J. P. (2024). Investigation of the Effect of Space Varying Wind Input on Hydrodynamic Modeling in Manila Bay and Laguna Lake, *The International Archives of the Photogrammetry, Remote Sensing and Spatial Information Sciences,* XLVIII-4/W8-2023, 143–148. https://doi.org/10.5194/isprs-archives-XLVIII-4-W8-2023-143-2024

Düzen, H. (2011). Van Gölü Su Seviye Değişimlerine Hidrojeolojik Yaklaşım, *66th Geological Concress of Turkey abstract book*, pp:264, 1-5 April 2013, TMMOB JMO, Ankara

Falconer, R. A. (1992). Flow and water quality modelling in coastal and inland water. *Journal of Hydraulic Research,* 30(4), 437–452. https://doi.org/10.1080/00221689209498893

Gill, A. E., (1982) *Atmospheric-Ocean Dynamics. International Geophysics Series* (1st ed.). Academic Press. https://doi.org/10.1016/S0074-6142(08)X6002-4

Holthuijsen, L.H. (2007). *Waves in Oceanic and Coastal Waters* (1st ed.). Cambridge University Press. https://doi.org/10.1017/CBO9780511618536

Kiran, N., Yenigün, O. Albek, E., & Börekçi, O. (1995). Wind-induced circulations of the Black Sea. *Water Science and Technology*, 32(7), 87-93. https://doi.org/10.1016/0273-1223(95)00051-8

Koçyiğit, M. B., & Koçyiğit, Ö. (2004). Numerical Study of Wind-Induced Currents in Enclosed Homogeneous Water Bodies. *Turkish Journal of Engineering and Environmental Sciences,* 28, 207–221, https://online-journals.tubitak.gov.tr/engineering/abstract.htm?id=7003

Koutitas, C. G. (1988). *Mathematical Models in Coastal Engineering* (1st ed.). Pentech Press Limited.

Matlab. (2022). MATLAB version: 9.13.0 (R2022b), Natick, Massachusetts: The MathWorks Inc. https://www.mathworks.com

Pope, S.B. (2000). *Turbulent Flows* (1st ed.). Cambridge University Press. https://doi.org/10.1017/CBO9781316179475

Pedlosky, J. (1987). *Geophysical Fluid Dynamics* (2nd ed.). Springer. https://doi.org/10.1007/978-1-4612-4650-3

Rodi, W. (1993). *Turbulence Models and Their Application in Hydraulics* (1st ed). Routledge. https://doi.org/10.1201/9780203734896

Santo, M. A., Toffolon, M., Zanier, G., Giovannini, L., & Armenio V., (2017). Large eddy simulation (LES) of wind-driven circulation in a peri-alpine lake: Detection of turbulent structures and implications of a complex surrounding orography. *Journal of Geophysical Research: Oceans,* 122, 4704–4722. https://doi.org/10.1002/2016JC012284

Sarı, M. (2000). *Bilinmeyen Van Gölü* (1. baskı). Alfa Yayınevi, 232 s.

Schoen, J. H., Stretch, D. D. & Tirok, K. (2014). Wind-driven circulation patterns in a shallow estuarine lake: St Lucia, South Africa, Estuarine. *Coastal and Shelf Science,* 146, 49-59, https://doi.org/10.1016/j.ecss.2014.05.007

Stockhecke, M., Kwiecien, O., Vigliotti, L., Anselmetti, F. S., Beer, J., Çağatay, M. N., Channell, J. E. T., Kipfer, R., Lachner, J., Litt, T., Pickarski, N., & Sturm, M. (2014). Chronostratigraphy of the 600,000-year-old continental record of Lake Van (Turkey). *Quaternary Science Reviews,* 104, 8-17. https://doi.org/10.1016/j.quascirev.2014.04.008

Stockhecke, M., Anselmetti, F.S, Meydan, A.F., Odermatt, D., & Sturm, M. (2012). The annual particle cycle in Lake Van (Turkey). *Palaeogeography, Palaeoclimatology, Palaeoecology,* 333, 148-159, https://doi.org/10.1016/j.palaeo.2012.03.022

Swatridge, L. L., Mulligan, R. P., Boegman, L., Shan, S., & Valipour, R. (2022). Coupled modelling of storm surge, circulation and surface waves in a large stratified lake. *Journal of Great Lakes Research,* 48(6), 1520-1535. https://doi.org/10.1016/j.jglr.2022.08.023

URL-1, 2024. Rüzgarlı dalgalar görseli. https://pixabay.com/tr/photos/r%C3%BCzg%C3%A2r-r%C3%BCzgarl%C4%B1-dalgalar-deniz-4754113/ Accessed 11.12.2024.

URL-2, 2024. Denizhaber, Fırtına Van Gölü'nde dev dalgalar oluşturdu https://www.denizhaber.com/firtina-van-golunde-dev-dalgalar-olusturdu Accessed 11.12.2024.

URL-3, 2024. Gezihocası, Türkiye'nin En Büyük Gölleri. https://www.gezihocasi.com/turkiyenin-en-buyuk-golleri/ Accessed 15.12.2024.

URL-4, 2024. Bilgiustam, Van Gölü ve Özellikleri. https://www.bilgiustam.com/van-golu-ve-ozellikleri/ Accessed 18.12.2024.

US Army Corps of Engineers. (2016). *HEC-RAS River Analysis System – 2D Modeling User's Manual* (version 6.0). https://www.hec.usace.army.mil/confluence/rasdocs/r2dum/latest

Yiğit, M. E., & Tuncer Uysal, E. (2023). The Mathematical Analysis of Non-Homogeneous Horizontal Flow Model for Salinization in the Gediz Delta (Izmir). In Atila Kumbasaroğlu (Eds), *Innovative Apporaches in Civil Engineering and Management Watershed-Based Water Research.* (pp: 43-63). BIDGE Publications Inc, Ankara. ISBN:978-625-6707-27-6

Yiğit M. E., & Yıldırım, M. S. (2025). *Analysis of the Transport of Domestic Wastewater Pollutants in Coastal Areas Using Mathematical Modeling: The Case of Izmir Bay.* 10th Azerbaijan Congress on Life, Engineering, Mathematical, and Applied Sciences Congress, (pp: 64-75) 13-15 Mart 2025, Baku, AZERBAIJAN.

Zafirakou A., Palantzas G., Karambas T., & Koutitas C. (2014). Optimization in oil slick combating stations allocation. Application to the Sea of Azov. *Global NEST Journal,* 16(2), 402-410. https://doi.org/10.30955/gnj.001335

Zafirakou, A., Palantzas, G., Samaras, A., & Koutitas, C. (2015). Oil Spill Modeling Aiming at the Protection of Ports and Coastal Areas. *Environmental Processes.* 2, 41–53. https://doi.org/10.1007/s40710-015-0100-8

Zhang, C., Chen, L., & Brett, M. T. (2024). Adaptation of wind drag coefficient parameterization: Improvement of hydrodynamic modeling by a wave-dependent Cd in large shallow lakes. *Water Resources Research,* 60, 1-17. https://doi.org/10.1029/2023WR035914